Two Microwave Vector Signal Transmission on a Single Optical Carrier Based on PM-IM Conversion Using an On-Chip Optical Hilbert Transformer

Yishi Han, Weifeng Zhang, *Student Member, IEEE*, Jiejun Zhang, *Student Member, IEEE*, and Jianping Yao, *Fellow, IEEE*

***Abstract*—A new microwave photonic link to simultaneously transmit and detect two microwave vector signals modulated on a single optical carrier based on orthogonal modulation and optical Hilbert transformation is proposed and demonstrated, for the first time to the best of our knowledge. In the proposed system, two microwave vector signals are phase and intensity modulated on a single optical carrier at a dual-parallel Mach–Zehnder modulator and transmitted over a single-mode fiber (SMF). At the receiver, the optical signal is applied directly to a photodetector (PD) to recover the microwave vector signal that is intensity modulated and the second microwave vector signal is recovered by using an on-chip optical Hilbert transformer (OHT) to perform phase-modulation to intensity-modulation conversion followed by photodetection at a second PD. An experiment is performed. The transmission of a 16QAM and a QPSK signal with a total data rate of 2.4 Gb/s over a 10-km SMF is implemented. The performance of the transmission in terms of error vector magnitude, bit error rate, and energy efficiency is evaluated.**

***Index Terms*—Optical Hilbert transformer, phase modulation to intensity modulation conversion, silicon microdisk resonator, vector signal generation.**

I. Introduction

THANKS to the low propagation loss, ultra-broad bandwidth and immunity to electromagnetic interference, microwave photonic links (MPLs) have been considered a good solution for wideband and low-loss microwave signal transmission and have found numerous applications such as in radio over fiber communications and antenna remoting [1], [2]. To meet the ever-increasing demand of higher-data-rate transmission, future wireless access networks are required to have a high spectrum efficiency to maximize the use of the limited spectrum resources. To reach this goal, advanced modulation formats can be used. These advanced modulated signals are vector signals, such as phase-shift keying (PSK) and quadrature-amplitude modulation (QAM). The combination of the MPL transmission technology and advanced signal modulation schemes can further enhance the data transmission capacity, which has become an active research topic recently [3]–[13].

To transmit a microwave vector signal over an optical fiber, a microwave vector signal is usually generated in the electrical domain and encoded on an optical carrier at an electro-optic modulator for transmission over an optical fiber [3]–[5]. Since the microwave vector signal generated in the electrical domain has a low microwave carrier frequency, to have a high carrier -frequency microwave vector signal, photonic techniques have been proposed [6]–[11]. For example, an optical heterodyning technique can be used to up-convert a low carrier-frequency microwave signal to a high carrier-frequency. However, the main problem associated with this technique is that only one microwave vector signal is carried by an optical carrier, which limits the spectrum efficiency. To have a high spectrum efficiency, it is highly preferred that multiple microwave vector signals could be carried by a single optical carrier and transmitted over a single optical fiber. Recently, we proposed two approaches to generate and transmit multiple vector microwave signals that are carried by a single optical carrier [12], [13]. In [12], two microwave vector signals are modulated on a single optical carrier and transmitted over a fiber at the transmitter. At the receiver, coherent detection using a local oscillator (LO) light source assisted with digital signal processing (DSP) is performed to recover the two microwave vector signals. To further enhance the spectrum efficiency [13], four microwave vector signals are modulated on a single optical carrier, and the detection of the four microwave vector signals is performed based on coherent detection and DSP using an advanced algorithm. Although coherent detection-based MPL could offer an increased spectral efficiency and improved receiver sensitivity, an expensive coherent receiver, an LO light source and a high-speed DSP unit are needed, which would make the system implementation complicated and costly.

Manuscript received September 29, 2017; revised November 16, 2017; accepted November 17, 2017. Date of publication November 21, 2017; date of current version February 24, 2018. This work was supported by the Natural Sciences and Engineering Research Council of Canada. The work of Y. Han was supported in part by the National Science Foundation of China under Grant 61471130, in part by the Science and Technology Planning Project of Guangdong Province, China, under Grant 2016B090918061, and in part by the Science and Technology Planning Project of Guangzhou City, China, under Grant 201604016079. *(Corresponding author: Jianping Yao.)*

Y. Han is with the Microwave Photonics Research Laboratory, School of Electrical Engineering and Computer Science, University of Ottawa, Ottawa, ON K1N 6N5, Canada, and also with the School of Information Engineering, Guangdong University of Technology, Guangzhou 510006, China (e-mail: yshan@gdut.edu.cn).

W. Zhang, J. Zhang, and J. Yao are with the Microwave Photonics Research Laboratory, School of Electrical Engineering and Computer Science, University of Ottawa, Ottawa, ON K1N 6N5, Canada (e-mail: jpyao@eecs.uottawa.ca).

Color versions of one or more of the figures in this paper are available online at http://ieeexplore.ieee.org.

Digital Object Identifier 10.1109/JLT.2017.2776276

To have a high spectrum efficiency while maintaining a simple configuration, in this paper we propose and demonstrate an MPL to simultaneously transmit two microwave vector signals modulated on a single optical carrier based on intensity and phase modulation and optical Hilbert transformation. In the proposed system, two independent microwave vector signals are phase and intensity modulated on a single optical carrier at a dual-parallel Mach-Zehnder modulator (DP-MZM) and transmitted over a single-mode fiber (SMF). At the receiver, the transmitted optical signal is split into two channels. One channel is applied directly to a photodetector (PD), and the microwave vector signal that is intensity modulated on the optical carrier is recovered. The other channel is sent to an on-chip optical Hilbert transformer (OHT) to perform phase-modulation to intensity-modulation conversion and is then detected at a second PD, and the microwave vector signal that is phase modulated on the optical carrier is recovered. The approach is analyzed theoretically and verified by an experiment. The transmission of a QPSK and 16QAM signal with a total date rate of 2.4 Gb/s over a 10-km SMF is demonstrated. In implementing the Hilbert transformation, to improve the power efficiency, a small frequency shift between the optical carrier and the notch center of the OHT is introduced, to avoid the optical carrier being suppressed. The transmission performance in terms of error vector magnitude (EVM) and bit error rate (BER) is evaluated. Compared with a conventional microwave vector signal transmission link, the key advantage of the proposed MPL is that the spectrum efficiency is doubled since two microwave vector signals carried by an optical carrier are simultaneously transmitted in a single optical fiber. In addition, thanks to the small frequency shift between the optical carrier and the notch center of the OHT, the optical carrier is not suppressed, and the power efficiency of the OHT is increased, which makes the transmission of the two microwave vectors signals have identical performance.

II. Principle of Operation

Fig. 1(a) shows the schematic diagram of the proposed MPL, in which two microwave vector signals carried by a single optical carrier over a single optical fiber are transmitted to a receiver where the vector signals are recovered with one by direct photodetection and the other through an OHT and then photodetection. In the transmitter, a continuous-wave (CW) optical signal generated by a laser diode (LD) is sent to a DP-MZM in which the optical signal is equally split into two channels with one being intensity modulated by a first microwave vector signal $I(t)$ at a sub-MZM (sub-MZM1) and the other being phase modulated by a second microwave vector signal $Q(t)$ in a second sub-MZM (sub-MZM2). Note that sub-MZM1 is biased at the quadrature point, thus a double-sideband intensity-modulated signal is generated. To achieve phase modulation, sub-MZM2 is biased at the null point, thus a double-sideband without carrier signal is generated. By applying a bias voltage to the main-MZM to introduce a π phase shift to the two sidebands, and by adding the optical carrier from sub-MZM1 to the two sidebands, an equivalent phase modulated signal is obtained [14]. Then, the combined phase- and intensity-modulated optical signals are transmitted

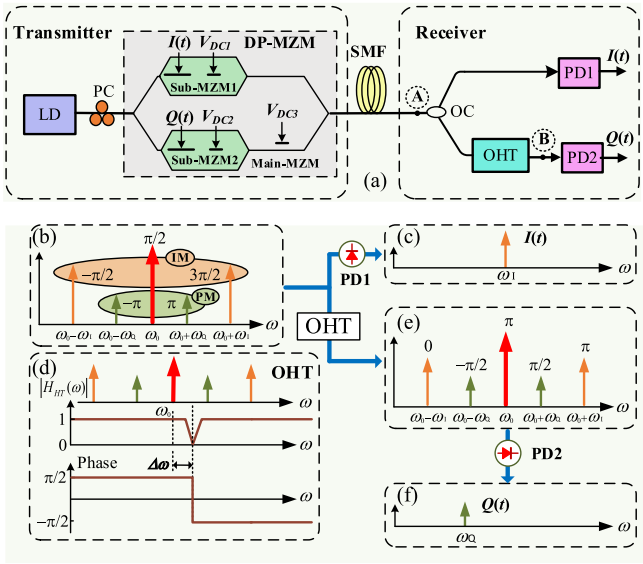

Fig. 1. Schematic diagram and operation principle of the proposed MPL. (a) Experimental setup. LD: laser diode; PC: polarization controller; OC, optical coupler; DP-MZM: dual-parallel Mach-Zehnder modulator; OHT: optical Hilbert transformer, PD: photodetector; SMF: single-mode fiber. (b) Optical spectrums of the intensity- and phase-modulated optical signals at the point A. (c) Recovered microwave vector signal $I(t)$ at the output of PD1. (d) Magnitude and phase responses of the OHT. (e) Optical spectrums of the modulated optical signals at the output the OHT at the point B. (f) Recovered microwave vector signal $Q(t)$ at the output of PD2.

to the receiver over a length of SMF. At the receiver, the optical signal is divided into two channels with one directly detected at a first PD (PD1), to recover the intensity-modulated signal $I(t)$. The other one is sent to an OHT to perform phase-modulation to intensity-modulation conversion. The PM-IM converted signal is then applied to a second PD (PD2) and the signal $Q(t)$ is recovered.

Mathematically, the optical carrier from the LD is written as

$$E_{\text{in}}(t) = E_0 e^{j\omega_0 t} \tag{1}$$

where E_0 is the amplitude and ω_0 is the angular frequency of the optical carrier.

The two microwave vector signals $I(t)$ and $Q(t)$ are applied to sub-MZM1 and sub-MZM2, respectively. Supposing that the vector signal $I(t)$ is a 16QAM signal and the vector signal $Q(t)$ is a QPSK signal, the two vector signals could be generally expressed as

$$I(t) = E_I(t)\cos\left[\omega_I t + \varphi_I(t)\right] \tag{2}$$

$$Q(t) = E_Q(t)\cos\left[\omega_Q t + \varphi_Q(t)\right] \tag{3}$$

where $E_I(t)$ is the amplitude, ω_I is the angular frequency, and $\varphi_I(t)$ is the phase of the microwave signal $I(t)$. $E_Q(t)$ is the amplitude, ω_Q is the angular frequency, and $\varphi_Q(t)$ is the phase of the microwave signal $Q(t)$.

The optical fields at the outputs of sub-MZM1 and sub-MZM2 are given by

$$E_{\text{out1}}(t) = \frac{1}{2}E_{\text{in}}(t)\sum_{n=-\infty}^{\infty} J_n\left[\beta_I(t)\right]e^{jn[\omega_I t+\varphi_I(t)+\pi]} \cos\left(\frac{\pi V_{DC1}}{2V_{\pi 1}}-\frac{n\pi}{2}\right) \tag{4}$$

And

$$E_{\text{out2}}(t) = \frac{1}{2}E_{\text{in}}(t)\sum_{n=-\infty}^{\infty} J_n\left[\beta_Q(t)\right]e^{jn[\omega_Q t+\varphi_Q(t)+\pi]} \cos\left(\frac{\pi V_{DC2}}{2V_{\pi 2}}-\frac{n\pi}{2}\right) \tag{5}$$

where $J_n[\beta_I(\mathrm{t})]$ and $J_n[\beta_Q(\mathrm{t})]$ are the Bessel functions of the first kind, $\beta_I(t)=\pi E_I(t)/(2V_{\pi 1})$ and $\beta_Q(t)=\pi E_Q(t)/(2V_{\pi 2})$ are the modulation indices, $V_{\pi 1}$ and $V_{\pi 2}$ are the half-wave voltages of sub-MZM1 and sub-MZM2, respectively, and V_{DC1} and V_{DC2} are the bias voltages applied to sub-MZM1 and sub-MZM2, respectively.

A bias voltage V_{DC3} is applied to the main-MZM to induce a phase shift to the modulated signal from sub-MZM1. At the output of the DP-MZM, the two optical signals are combined and the optical field could be written as

$$\begin{aligned} E_{\text{out}}(t) &= E_{\text{out1}}(t)\,e^{[j(\pi\frac{V_{DC3}}{V_{\pi DC}})]}+E_{\text{out2}}(t) \\ &= \frac{E_{\text{in}}(t)}{2}\begin{Bmatrix} \sum_{n=-\infty}^{\infty} J_n\left[\beta_{\text{I}}(t)\right]e^{jn[\omega_I t+\varphi_I(t)+\pi]} \\ \quad\cos\left(\frac{\pi V_{DC1}}{2V_{\pi 1}}-\frac{n\pi}{2}\right)e^{[j(\pi\frac{V_{DC3}}{V_{\pi DC}})]} \\ +\sum_{n=-\infty}^{\infty} J_n\left[\beta_{\text{Q}}(t)\right]e^{jn[\omega_Q t+\varphi_Q(t)+\pi]} \\ \quad\cos\left(\frac{\pi V_{DC2}}{2V_{\pi 2}}-\frac{n\pi}{2}\right) \end{Bmatrix} \end{aligned} \tag{6}$$

where $V_{\pi DC}$ is the half-wave voltage of the main-MZM. To realize double-sideband with carrier modulation for the microwave vector signal $I(t)$, sub-MZM1 is biased at the quadrature point with $V_{DC1}=V_{\pi 1}/2$. For the microwave vector signal $Q(t)$, equivalent phase modulation should be performed, which is done by biasing sub-MZM2 at the null point with $V_{DC2}=V_{\pi 2}$ to generate a double-sideband without carrier signal. By biasing the main-MZM at the quadrature point with $V_{DC3}=V_{\pi DC}/2$ to introduce a π phase shift to the two sidebands, and by adding the optical carrier from sub-MZM1 to the two sidebands, an equivalent phase modulated signal is obtained [14]. Since the small-signal modulation is assumed, the higher order ($\geq$2) sidebands are ignored. The optical field at the output of the DP-MZM can be simplified as

$$\begin{aligned} E_{\text{out}}(t) &= E_{\text{out1}}(t)\,e^{[j(\pi\frac{V_{DC3}}{V_{\pi DC}})]}+E_{\text{out2}}(t) \\ &\approx \frac{E_{\text{in}}(t)}{2}\begin{Bmatrix} \frac{\sqrt{2}}{2}J_0\left[\beta_{\text{I}}(t)\right]e^{j\left(\frac{\pi}{2}\right)} \\ \quad+\frac{\sqrt{2}}{2}J_{+1}\left[\beta_{\text{I}}(t)\right]e^{j[\omega_I t+\varphi_I(t)+\frac{3\pi}{2}]} \\ \quad-\frac{\sqrt{2}}{2}J_{-1}\left[\beta_{\text{I}}(t)\right]e^{-j[\omega_I t+\varphi_I(t)+\frac{\pi}{2}]} \\ \quad+J_{+1}\left[\beta_{\text{Q}}(t)\right]e^{j[\omega_Q t+\varphi_Q(t)+\pi]} \\ \quad-J_{-1}\left[\beta_{\text{Q}}(t)\right]e^{-j[\omega_Q t+\varphi_Q(t)+\pi]} \end{Bmatrix} \end{aligned} \tag{7}$$

Since the microwave signal is much smaller than the half-wave voltage of the DP-MZM, we have $J_0[\beta_I(\mathrm{t})]\approx 1$. Eq. (7) can be further rewritten as

$$\begin{aligned} E_{\text{out}}(t) &= E_{\text{out1}}(t)\,e^{[j(\pi\frac{V_{DC3}}{V_{\pi DC}})]}+E_{\text{out2}}(t) \\ &\approx \frac{E_{\text{in}}(t)}{2}\begin{Bmatrix} \frac{\sqrt{2}}{2}e^{j\left(\frac{\pi}{2}\right)} \\ \quad+\frac{\sqrt{2}}{2}J_{+1}\left[\beta_{\text{I}}(t)\right]e^{j\left[\omega_I t+\varphi_I(t)+\frac{3\pi}{2}\right]} \\ \quad-\frac{\sqrt{2}}{2}J_{-1}\left[\beta_{\text{I}}(t)\right]e^{-j\left[\omega_I t+\varphi_I(t)+\frac{\pi}{2}\right]} \\ \quad+J_{+1}\left[\beta_{\text{Q}}(t)\right]e^{j[\omega_Q t+\varphi_Q(t)+\pi]} \\ \quad-J_{-1}\left[\beta_{\text{Q}}(t)\right]e^{-j[\omega_Q t+\varphi_Q(t)+\pi]} \end{Bmatrix} \end{aligned} \tag{8}$$

The combined optical signals are transmitted over a length of SMF. Fig. 1(b) shows the optical spectrums of the modulated optical signals after the transmission over a length of SMF at point A in Fig. 1(a). The phase relationship between the optical carrier and the two sidebands shows the microwave signal $I(t)$ is intensity modulated, and the microwave signal $Q(t)$ is phase modulated. By applying the optical signals directly to a PD (PD1), only the intensity-modulated signal will be detected. The current at the output of the PD could be written as

$$\begin{aligned} I_A(t) &= \Re\left[E_{\text{out}}(t)\times E_{\text{out}}^{*}(t)\right] \\ &\approx \frac{1}{4}\Re P_0\begin{Bmatrix} \frac{1}{2}+\frac{1}{2}J_{+1}\left[\beta_{\text{I}}(t)\right]e^{j[\omega_I t+\varphi_I(t)]} \\ -\frac{1}{2}J_{-1}\left[\beta_{\text{I}}(t)\right]e^{-j[\omega_I t+\varphi_I(t)]} \end{Bmatrix} \end{aligned} \tag{9}$$

where $\Re$ is the photon responsivity of PD1, and P_0 is the optical power of the carrier. Using the relation $J_{+1}[\beta_I(t)]=-J_{-1}[\beta_I(t)]$, the current at the output of the PD1 could be further rewritten as

$$I_A(t)\approx\frac{1}{4}\Re P_0\left\{\frac{1}{2}+J_{+1}\left[\beta_{\text{I}}(t)\right]\cos\left[\omega_I t+\varphi_I(t)\right]\right\} \tag{10}$$

Thanks to the intensity modulation of $I(t)$ and phase modulation of $Q(t)$, only the vector microwave signal $I(t)$ is recovered at the output of PD1 and no microwave signal $Q(t)$ is detected, as shown in Fig. 1(c). The reason is that when a phase-modulated optical signal is applied to a PD, the beating between the optical carrier and the upper sideband will fully cancel the beating between the optical carrier and the lower sideband.

To recover the vector signal $Q(t)$, the output signal $E_{\text{out}}(\mathrm{t})$ is sent to an OHT, to perform PM-IM conversion. The frequency response of an OHT is given by

$$H_{\text{OHT}}(\omega)=\begin{cases} e^{-j\pi/2}, & \omega>\omega_0+\Delta\omega \\ 0, & \omega=\omega_0+\Delta\omega \\ e^{j\pi/2}, & \omega<\omega_0+\Delta\omega \end{cases} \tag{11}$$

where $\Delta\omega$ is the frequency shift between the optical carrier and the notch center of the OHT, and ω_0 is again the angular frequency of the optical carrier.

Fig. 1(d) shows the magnitude and phase responses of an OHT. As can been, a notch is located at the center of the magnitude response and a π phase shift is seen at the center of the phase response. The optical carrier is slightly away from the center of the notch by $\Delta\omega$. When a phase-modulated optical

signal is applied to the OHT, a $\pi/2$ phase shift is introduced to the lower sideband and the optical carrier, and a $-\pi/2$ phase shift is introduced to the upper sideband. The phase modulated signal is then converted to an intensity-modulated signal.

Since the optical carrier is located away from the notch center of the OHT, as shown in Fig. 1(d), the optical power of the optical carrier is not suppressed, which leads to an increased power efficiency. At the output of the OHT, the transmitted optical signal could be written as

$$E_{\text{out}}(t) = \frac{E_{\text{in}}(t)}{2}\left\{\begin{array}{l}\frac{\sqrt{2}}{2}e^{j\pi}+\frac{\sqrt{2}}{2}J_{+1}\left[\beta_{\text{I}}(t)\right]e^{j\left[\omega_I t+\varphi_I(t)+\pi\right]}\\ -\frac{\sqrt{2}}{2}J_{-1}\left[\beta_{\text{I}}(t)\right]e^{-j\left[\omega_I t+\varphi_I(t)\right]}\\ +J_{+1}\left[\beta_{\text{Q}}(t)\right]e^{j\left[\omega_Q t+\varphi_Q(t)+\frac{\pi}{2}\right]}\\ -J_{-1}\left[\beta_{\text{Q}}(t)\right]e^{-j\left[\omega_Q t+\varphi_Q(t)+\frac{\pi}{2}\right]}\end{array}\right\} \quad (12)$$

By observing the phase relationship between the two sidebands and the optical carrier, shown in Fig. 1(e), at the output of the OHT, the phase-modulated signal is converted to an intensity-modulated signal, and the intensity-modulated signal is converted to a phase-modulated signal. By applying the converted optical signals to a PD (PD2), the current at the output of PD2 is

$$I_A(t) \approx \frac{1}{4}\Re P_0\left\{\frac{1}{2}+J_{+1}\left[\beta_Q(t)\right]\cos\left[\omega_Q t+\varphi_Q(t)\right]\right\} \quad (13)$$

Thanks to the Hilbert transformation, microwave vector signal $Q(t)$ is recovered, as shown in Fig. 1(f).

Based on PM-IM conversion using an OHT, two microwave vector signals on a single optical carrier are simultaneously transmitted and recovered. In the analysis, the two microwave vector signals are considered a 16QAM and a DPSK signal, the proposed MPL still works when the microwave vector signals with other modulation formats are employed. The key advantage of the proposed method is that the spectrum efficiency is doubled since two microwave vector signals on a single optical carrier are transmitted. In addition, compared with conventional Hilbert transformation [15], [16], in which the optical carrier has to be placed at the notch, the power efficiency of the OHT is significantly enhanced since a small frequency shift between the optical carrier and the notch center of the OHT is introduced, to avoid the bandstop filtering of the optical carrier. Thus, no optical amplifier is needed at the output of the OHT to boost up the power of the recovered microwave vector signal, to make the two recovered microwave vector signals in the two channels have similar transmission performance.

III. Experiment and Discussion

A proof-of-concept experiment based on the setup in Fig. 1(a) is performed. A light wave from a tunable laser source (TLS, Anritsu MG9638A) with a linewidth of about 100 kHz and an output power of 15 dBm is sent to the DP-MZM (Fujitsu FTM7980EDA) via a polarization controller (PC). The PC is used to adjust the state of polarization of the incident light to minimize the polarization-dependent loss. The DP-MZM has a bandwidth of 10 GHz and a half-wave voltage of about

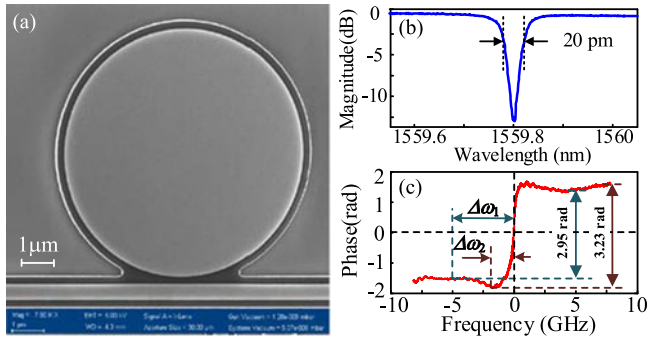

Fig. 2. (a) SEM micrograph of the fabricated MDR. (b) Measured transmission response of the fabricated MDR. (c) Measured phase response of the fabricated MDR, where $\Delta\omega_1 = 5$ GHz, $\Delta\omega_2 = 2$ GHz.

6.3 V. Two microwave vector signals are applied to the two sub-MZMs in the DP-MZM to modulate the optical carrier. The two microwave vector signals (16QAM and QPSK) have an identical center frequency of 10 GHz and an identical symbol rate of 400-MSymbol/s, which are generated by an arbitrary waveform generator (Keysight M8195A). By biasing sub-MZM1 and sub-MZM2 at the quadrature and null point, respectively, and biasing the main-MZM at the quadrature point, the 16QAM and QPSK signals are intensity- and phase- modulated on the optical carrier, respectively. At the output of the DP-MZM, the modulated optical signals are combined and transmitted over a 10-km SMF. At the receiver, the modulated optical signals are split equally into two channels using an optical coupler (OC) with a splitting ratio of 50:50. In the upper channel, the optical signals are sent to a 10-GHz photodetector (PD1) directly, and the 16QAM signal is recovered since it is intensity modulated. In the lower channel, the optical signals are sent to a silicon-based on-chip microdisk resonator (MDR), which functions as an OHT to perform Hilbert transformation. After the MRD, the optical signals are detected at another 10-GHz photodetector (PD2), and only the QPSK signal is recovered since it is converted to an intensity-modulated signal and the 16QAM signal cannot be detected since it is converted to a phase-modulated signal. A real-time oscilloscope (Keysight DSOZ504A) is used to simultaneously monitor the detected microwave vector signals from the outputs of the two channels.

In the experiment, a specifically-designed MDR is used for the implementation of the OHT. Fig. 2(a) gives the SEM micrograph of the fabricated MDR. The distinct feature of the MDR is that an additional slab waveguide is used to wrap the disk and bus waveguide to weaken the sidewall roughness on the confined optical field, which is of help to elevate the optical confining capacity of the MDR [17], [18]. The coupling gap between the disk and bus waveguide is carefully designed to make the MDR work in the critical coupling condition. Thus, a π phase shift would be achieved in the phase response of the notch, which is critical for implementation of an OHT using the MDR. Fig. 2(b) and (c) shows the magnitude and phase responses of the MDR around the resonance wavelength of 1559.803 nm measured using the optical single sideband (OSSB) modulation approach with a 40-GHz electronic vector network analyzer (EVNA) (Agilent

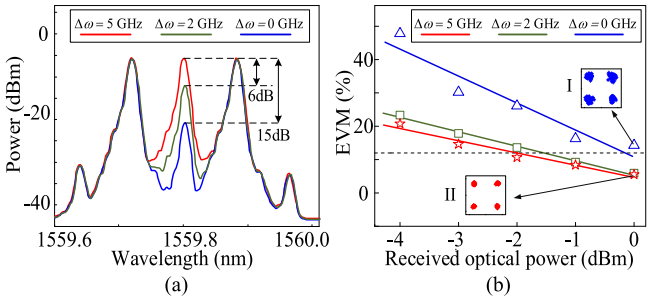

Fig. 3. (a) Measured optical spectrums of the transmitted optical signal after passing the OHT with a different frequency shift $\Delta\omega$. (b) Measured EVMs with three different frequency shifts at different received optical power levels. Insets show the constellations for the recovered QPSK microwave vector signals.

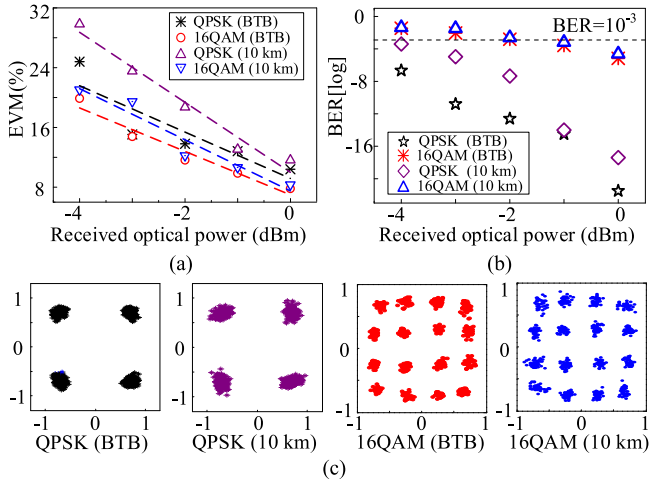

Fig. 4. (a) Measured EVMs and (b) BERs at different received optical power levels for the QPSK and 16QAM microwave vector signals. (c) Measured constellations for the recovered microwave vector signals at a received optical power of 0 dBm.

N5230A) [19]. The 3-dB bandwidth of the MDR is measured to be around 20 pm, corresponding to a Q-factor of 78,000, and the phase shift at the notch center of the MDR is measured to be 3.08 rad, which is very close to the ideal π phase shift.

Since the optical carrier has a frequency shift from the notch center of the OHT, the optical carrier is located out of the notch center. Thus, most of the optical carrier power is maintained after the OHT, which is of help to have a higher power efficiency. Thus, no optical amplifier is needed at the output of the OHT to boost up the power of the recovered microwave vector signal, to make the two recovered microwave vector signals have similar transmission performance.

We first evaluate the system performance in the term of EVMs for the phase-modulated QPSK signal when the Hilbert transformation is performed with different frequency shift $\Delta\omega$. The microwave carrier frequency is 10 GHz. By tuning the wavelength of the optical carrier, the frequency shift $\Delta\omega$ between the optical carrier and the notch center of the OHT is tuned. Fig. 3(a) shows the measured optical spectrum of the transmitted optical signal after the OHT with different frequency shifts. When the frequency shift $\Delta\omega$ is 0 GHz, the optical carrier is located in the notch center, which causes a heavy suppression of the optical carrier and thus a low power efficiency is resulted. When the frequency shift $\Delta\omega$ is 2 GHz, the optical carrier moves a little out of the notch center, the optical carrier has a power of 6 dBm smaller than the first-order sidebands. When the frequency shift $\Delta\omega$ is 5 GHz, the optical carrier has the same power as the first-order sidebands. Fig. 3(b) shows the measured EVMs for the QPSK microwave vector signal with the corresponding frequency shifts at the different received optical power levels. As can be seen, when the frequency shift $\Delta\omega$ is 0 GHz, due to a heavy suppression of the optical carrier after the OHT, the measured EVM at 0 dBm is larger than 12% and degrades significantly as the receiver optical power decreases. When the frequency shift $\Delta\omega$ is 5 GHz, the measured EVMs become much smaller and have a slow growth with the received optical power decreasing. Inset (I) and (II) in Fig. 3(b) shows the measured constellations for the recovered QPSK microwave vector signals at a received optical power of 0 dBm when the frequency shift $\Delta\omega$ is 0 and 5 GHz, respectively. Compared the two constellations, the constellation when the frequency shift $\Delta\omega$ is 5 GHz is much clearer. These experimental results confirm the effectiveness of the proposed OHT and high power efficiency when a frequency shift between the optical carrier and the notch center of the OHT is introduced.

We then evaluate the system performance in terms of the EVMs and BERs for the transmission of a phase-modulated QPSK signal and an intensity-modulated 16QAM signal. The microwave carrier frequencies for the two signals are identical, which are 10 GHz. The frequency shift $\Delta\omega$ for the evaluation is controlled at 5 GHz. In the proposed MPL system, the symbol rate for each of the digitally modulated microwave signal is 400-MSymbol/s, or a bit rate for the 16QAM microwave vector signal is 1.6 Gb/s and for the QPSK microwave vector signal is 0.8 Gb/s, and the total bit rate for the entire system is 2.4 Gb/s. Fig. 4(a) and (b) shows the measured EVMs and BERs of the two vector signals for back-to-back (BTB) and 10-km SMF transmission at a received optical power from -4 to 0 dBm. As can be seen in Fig. 4(a), with the received optical power increasing, the EVMs are improved since the signal-to-noise ratio (SNR) of the received signal is increased. Especially, when the received optical power is larger than -2 dBm, the measured EVMs for the QPSK and 16QAM signals after a 10-km SMF transmission is almost the same as the ones for BTB transmission. Similar result can also be found in the BER measurement shown in Fig. 4(b). When the received optical power is larger than -2 dBm, the measured BERs for the recovered microwave signal after a 10-km SMF transmission are still less than 3×10^{-3}, which ensures error-free transmission when forward error correction is employed [20]. Fig. 4(c) gives the measured constellation diagrams of the QPSK and 16QAM vector signals for BTB and 10-km SMF transmission at a received optical power of 0 dBm. As can be seen, the constellations are clear and no significant deterioration is presented. Note, a difference in the measured EVMs and BERs between the two microwave vector signals is observed, this is caused due to a large

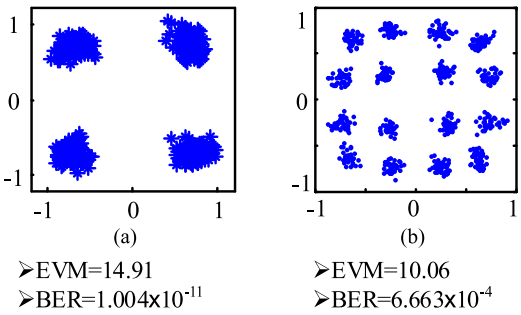

Fig. 5. Measured constellations for the recovered (a) QPSK and (b) 16QAM vector signals at an identical microwave carrier frequency of 6 GHz after transmission over a 10-km SMF. The received optical power is 0 dBm.

insertion loss resulted from the fiber-to-chip and chip-to-fiber coupling.

One important feature of the proposed MPL is that no electronic or optical filters are employed, which allows the frequency of the transmitted microwave vector signals to be tuned in a broad range. To evaluate the tunability, two new microwave vector signals having a new and identical carrier frequency of 6 GHz are generated and transmitted over a 10-km SMF transmission. Fig. 5 shows the measured constellations, EVMs and BERs for the two signals when the received optical power is 0 dBm. The measured EVMs and BERs have the similar values as those when the carrier frequency of the microwave signals is 10 GHz, and the constellations are also clear, which confirms the effectiveness of the MPL for the transmission of microwave vector signals at different microwave carrier frequencies. The minimum microwave carrier frequency of a microwave vector signal in our proposed MPL is determined by the 3-dB bandwidth of the MDR, and the maximum microwave carrier frequency is determined by the bandwidth of the DP-MZM, which is 10 GHz in the experiment. Therefore, the frequency range of the microwave vector signals that could be transmitted in the MPL is from 2.5 to 10 GHz. To further increase the frequency, a DP-MZM with a broader bandwidth should be used.

IV. Conclusion

We proposed and experimentally demonstrated an MPL to simultaneously transmit two microwave vector signals on a single optical carrier based on intensity modulation and phase modulation and optical Hilbert transformation. The detection of the phase-modulated vector signal at the receiver was realized using an OHT to convert the phase-modulated signal to an intensity-modulated signal. In addition, in implementing the OHT, a frequency shift was introduced between the optical carrier frequency and the notch center of the OHT, to increase the power efficiency of Hilbert transformation. The effectiveness of the proposed MPL was evaluated by an experiment. The transmission of two microwave vector signals on a single optical carrier with a total date rate of 2.4-Gb/s transmitted over a 10-km SMF was demonstrated. The transmission performance in terms of EVM and BER was evaluated. Compare with a conventional microwave vector signal transmission link, the key advantage of the proposed method is that the spectrum efficiency is doubled. In addition, thanks to the small frequency shift between the optical carrier and the notch center of the OHT, a high power efficiency was achieved. The proposed technique can be combined with other techniques, such as polarization multiplexing, to further increase the spectrum efficiency.

References

[1] J. Beas, G. Castanon, I. Aldaya, A. Zavala, and G. Campuzano, "Millimeter-wave frequency radio over fiber systems: A survey," *IEEE Commun. Surv. Tuts.*, vol. 15, no. 4, pp. 1593–1619, Mar. 2013.

[2] J. P. Yao, "Microwave photonics," *J. Lightw. Technol.*, vol. 27, no. 3, pp. 314–335, Feb. 3, 2009.

[3] Y. Chi, Y. Li, H. Wang, P. Peng, H. Lu, and G. Lin, "Optical 16QAM-52-OFDM transmission at 4 Gbit/s by directly modulating a coherently injection-locked colorless laser diode," *Opt. Express*, vol. 20, no. 18, pp. 20071–20077, Aug. 2012.

[4] I. S. Amiri, S. E. Alavi, S. M. Idrus, A. S. Supaat, J. Ali, and P. P. Yupapin, "W-Band OFDM transmission for radio-over-fiber link using solitonic millimeter wave generated by MRR," *IEEE J. Quantum Electron.*, vol. 50, no. 8, pp. 622–628, Aug. 2014.

[5] A. Kanno *et al.*, "All-spectrum fiber-wireless transmission for 5G backhaul and fronthaul links," in *Proc. Opt. Fiber Commun. Conf.*, Anaheim, CA, USA, 2016, Paper no. Th2A.26.

[6] R. Li, W. Li, X. Chen, and J. Yao, "Millimeter-wave vector signal generation based on a bi-directional use of a polarization modulator in a Sagnac loop," *J. Lightw. Technol.*, vol. 33, no. 1, pp. 251–257, Jan. 2015.

[7] Y. Zhang *et al.*, "Photonic DPASK/QAM signal generation at microwave/millimeter-wave band based on an electro-optic phase modulator," *Opt. Express*, vol. 33, no. 20, pp. 2332–2334, Oct. 2008.

[8] L. Huang, Z. Tang, P. Xiang, W. Wang, S. Pan, and X. Chen, "Photonic generation of equivalent single sideband vector signals for RoF systems," *IEEE Photon. Technol. Lett.*, vol. 28, no. 22, pp. 2633–2636, Nov. 2016.

[9] X. Li *et al.*, "QAM vector signal generation by optical carrier suppression and precoding techniques," *IEEE Photon. Technol. Lett.*, vol. 27, no. 18, pp. 1977–1980, Sep. 2015.

[10] C. Lin, P. Shih, W. Jiang, E. Wong, J. J. Chen, and S. Chi, "Photonic vector signal generation at microwave/millimeter-wave bands employing an optical frequency quadrupling scheme," *Opt. Lett.*, vol. 34, no. 14, pp. 2171–2173, Jul. 2009.

[11] X. Li, J. Zhang, J. Xiao, Z. Zhang, Y. Xu, and J. Yu, "W-band 8QAM vector signal generation by MZM-based photonic frequency octupling," *IEEE Photon. Technol. Lett.*, vol. 27, no.12, pp. 1257–1260, Jun. 2015.

[12] Y. Chen, T. Shao, A. Wen, and J. Yao, "Microwave vector signal transmission over an optical fiber based on IQ modulation and coherent detection," *Opt. Lett.*, vol. 39, no. 6, pp. 1509–1512, Mar. 2014.

[13] X. Chen and J. Yao, "4 × 4 multiple-input multiple-output coherent microwave photonic link with optical independent sideband and optical orthogonal modulation," *Chin. Opt. Lett.*, vol. 15, no. 1, Jan. 2017, Paper no. 010008.

[14] X. Han and J. P. Yao, "Tunable single bandpass microwave photonic filter with an improved dynamic range," *IEEE Photon. Technol. Lett.*, vol. 28, no. 1, pp. 11–14, Jan. 2016.

[15] T. X. H. Huang, X. Yi, and R. A. Minasian, "Microwave photonic quadrature filter based on an all-optical programmable Hilbert transformer," *Opt. Lett.*, vol. 36, no. 22, pp. 4440–4442, Nov. 2011.

[16] Y. Cao, E. H. W. Chan, X. Wang, X. Feng, and B. Guan, "Photonic microwave quadrature filter with low phase imbalance and high signal-to-noise ratio performance," *Opt. Lett.*, vol. 40, no. 20, pp. 4663–4666, Oct. 2015.

[17] W. Zhang and J. Yao, "Silicon-based on-chip microdisk resonators for integrated microwave photonic applications," in *Proc. Opt. Fiber Commun. Conf.*, Anaheim, CA, USA, 2016, Paper no M2B.6.

[18] W. Zhang and J. P. Yao, "Silicon-based single-mode on-chip ultra-compact microdisk resonator," *J. Lightw. Technol.*, vol. 35, no. 20, pp. 4418–4424, Oct. 2017.

[19] Z. Tang, S. Pan, and J. Yao, "A high resolution optical vector network analyzer based on a wideband and wavelength tunable optical single-sideband modulator," *Opt. Express*, vol. 20, no. 6, pp. 6555–6560, Mar. 2012.

[20] R. Schmogrow *et al.*, "512QAM Nyquist sinc-pulse transmission at 54 Gbit/s in an optical bandwidth of 3 GHz," *Opt. Express*, vol. 20, no. 6, pp. 6439–6447, Mar. 2012.

Yishi Han received the Ph.D. degree in optical engineering from Zhejiang University, Hangzhou, China, in 2004.

In 2004, he joined the School of Information Engineering, Guangdong University of Technology, Guangzhou, China, as a Lecturer, where he became a Professor in 2014. He is currently a Visiting Scholar in the Microwave Photonics Research Laboratory, School of Electrical Engineering and Computer Science, University of Ottawa, ON, Canada. His current research interests include microwave photonics and radio-over-fiber communications.

Weifeng Zhang (S'12) received the B.Eng. degree in electronic science and technology from Xi'an Jiaotong University, Xi'an, China, in 2008, the M.A.Sc. degree in electrical engineering from the Polytechnic University of Turin, Turin, Italy, in 2011, and the Ph.D. degree in electrical engineering from the University of Ottawa, Ottawa, ON, Canada.

He is currently a Postdoctoral Fellow with the Microwave Photonics Research Laboratory, School of Electrical Engineering and Computer Science, University of Ottawa. His current research interests include silicon photonics and its applications in microwave photonics

Jiejun Zhang (S'12) received the B.Eng. degree in electronic science and technology from Harbin Institute of Technology, Harbin, China, in 2010, the M.Sc. degree in optical engineering from Huazhong University of Science and Technology, Wuhan, China, and the Ph.D. degree in electrical engineering from the Microwave Photonics Research Laboratory, School of Electrical Engineering and Computer Science, University of Ottawa, Ottawa, Canada, in 2017.

His research interests include photonic generation of microwave waveforms, photonic processing of microwave signals, and fiber optic sensors.

Jianping Yao (M'99–SM'01–F'12) received the Ph.D. degree in electrical engineering from the Université de Toulon et du Var, Toulon, France, in December 1997. From 1998 to 2001, he was an Assistant Professor with the School of Electrical and Electronic Engineering, Nanyang Technological University, Singapore. In December 2001, he was an Assistant Professor with the School of Electrical Engineering and Computer Science, University of Ottawa, where he was promoted to an Associate Professor in 2003 and a Full Professor in 2006. In 2007, he was appointed as a University Research Chair in Microwave Photonics. From July 2007 to June 2010 and from July 2013 to June 2016, he was the Director of the Ottawa-Carleton Institute for Electrical and Computer Engineering. He is currently a Professor and the University Research Chair with the School of Electrical Engineering and Computer Science, University of Ottawa, Ottawa, ON, Canada. He has authored or coauthored more than 520 research papers, including more than 310 papers in peer-reviewed journals and 210 papers in conference proceedings Dr. Yao is an Editor-in-Chief for IEEE PHOTONICS TECHNOLOGY LETTERS, a Topical Editor for *Optics Letters*, and serves on the Editorial Boards of the IEEE TRANSACTIONS ON MICROWAVE THEORY AND TECHNIQUES, *Optics Communications*, *Frontiers of Optoelectronics*, and *Science Bulletin*. He was as a Guest Co-Editor for a focus issue on microwave photonics in *Optics Express* in 2013 and a Lead-Editor for a feature issue on microwave photonics in *Photonics Research* in 2014. He is a Chair of numerous international conferences, symposia, and workshops, including the Vice Technical Program Committee (TPC) Chair of the IEEE Microwave Photonics Conference in 2007, a TPC Co-Chair of the Asia-Pacific Microwave Photonics Conference in 2009 and 2010, a TPC Chair of the high-speed and broadband wireless technologies subcommittee of the IEEE Radio Wireless Symposium in 2009–2012, a TPC Chair of the microwave photonics subcommittee of the IEEE Photonics Society Annual Meeting in 2009, a TPC Chair of the IEEE Microwave Photonics Conference in 2010, a General Co-Chair of the IEEE Microwave Photonics Conference in 2011, a TPC Co-Chair of the IEEE Microwave Photonics Conference in 2014, and a General Co-Chair of the IEEE Microwave Photonics Conference in 2015. He is also a committee member of numerous international conferences, such as IPC, OFC, BGPP, and MWP. He was an IEEE MTT-S Distinguished Microwave Lecturer for 2013–2015. He is a registered Professional Engineer of Ontario. He is a Fellow of the OSA, and the Canadian Academy of Engineering CAE. In June 2016, he was conferred the title of Distinguished University Professor of the University of Ottawa. He was recipient of the 2005 International Creative Research Award of the University of Ottawa, the 2007 George S. Glinski Award for Excellence in Research, and a Natural Sciences and Engineering Research Council of Canada Discovery Accelerator Supplements Award in 2008. He was selected to receive an inaugural OSA Outstanding Reviewer Award in 2012.